Ab initio calculation of low-energy collective charge-density excitations in MgB_2

V. M. Silkin,[1,2,3] A. Balassis,[2,4] P. M. Echenique,[1,2] and E. V. Chulkov[1,2]
[1]*Depto. de Física de Materiales and Centro Mixto CSIC–UPV/EHU, Facultad de Ciencias Químicas, Universidad del País Vasco, Apdo. 1072, 20080 San Sebastián, Basque Country, Spain*
[2]*Donostia International Physics Center (DIPC), P. Manuel Lardizabal 4, 20018 San Sebastián, Basque Country, Spain*
[3]*IKERBASQUE, Basque Foundation for Science, 48011, Bilbao, Spain*
[4]*Physics Department, Fordham University, 441 East Fordham Road, Bronx NY 10458-5198, USA*
(Dated: September 6, 2009)

We present *ab-initio* time-dependent density-functional theory calculation results for low-energy collective electron excitations in MgB_2. The existence of a long-lived collective excitation corresponding to coherent charge density fluctuations between the boron σ- and π- bands ($\sigma\pi$ mode) is demonstrated. This mode has a sine-like oscillating dispersion for energies below 0.5 eV. At even lower energy we find another collective mode ($\sigma\sigma$ mode). We show the strong impact of local-field effects on dielectric functions in MgB_2. These effects account for the long q-range behavior of the modes. We discuss the physics that these collective excitations bring to the energy region typical for lattice vibrations.

PACS numbers: 74.25.Kc,71.45.Gm,73.43.Lp,74.70.Ad

After several years of intense experimental and theoretical study of the origin of unusually high temperature superconductivity[1] in MgB_2, nowadays there is a general belief that the superconductivity in MgB_2 is phonon-mediated with multiple gaps and an exceptional role played by E_{2g} phonon mode in strong coupling to electrons in the tubular-shaped σ bands at the Fermi level, E_F. However, despite the tremendous progress achieved in understanding of superconductivity in MgB_2, many of its fundamental properties related to phonons and electron-phonon ($e-ph$) coupling are still puzzling and remain under intense debate. Thus such important issues as, e.g., the reduced isotope effect,[2,3,4] the nature of the strong broad continuum in Raman spectra, the unusually broad linewidth of the E_{2g} phonon mode seen in Raman spectra,[5,6,7] the inconsistency between the results of Raman scattering and x-ray measurements,[8,9,10] and the role of non-adiabatic effects[8,11,12,13,14] have not yet found satisfactory explanations.

As for the electronic part of the $e-ph$ picture of superconductivity in MgB_2, it has received substantially less attention than the phonon part. In particular, in all evaluations of the $e-ph$ interaction the adiabatic approximation has been used, and even in *ab initio* calculations[15] of T_c the dynamical Coulomb interaction has been considered in its static form. Here we present a detailed *ab initio* study of the low-energy dynamical electronic properties of MgB_2. We demonstrate that the strongly anisotropic electronic structure of MgB_2 characterized by boron quasi two-dimensional σ and three-dimensional π bands[16,17] leads to remarkable low-energy dielectric response in this compound: collective modes with a peculiar sine-like oscillating dispersion appear in the 0-0.5 eV energy range. This brings interesting physics to the energy region which was thought to be entirely dominated by lattice vibrations.

Our approach is based on time-dependent density functional theory[18] where the non-local dynamical density-response function, χ, determines an induced charge density, ρ, in the electronic system caused by an external potential, $v_{\rm ext}$, according to

$$\rho(\mathbf{r},t)=\int \chi(\mathbf{r},t;\mathbf{r}',t')\,v_{\rm ext}(\mathbf{r}',t')\,{\rm d}\mathbf{r}'{\rm d}t'. \qquad (1)$$

χ is obtained from the integral equation $\chi=\chi^o+\chi^o(v+K_{\rm xc})\chi$, where $\chi^o(\mathbf{r},t;\mathbf{r}',t')$ is the response function of non-interacting electron system, $v(\mathbf{r}-\mathbf{r}')$ is the bare Coulomb potential, and $K_{\rm xc}$ accounts for dynamical exchange-correlation effects. In terms of Fourier-transformed quantities the imaginary part of the matrix $\chi^o_{\mathbf{GG}'}(\mathbf{q},\omega)$ can be evaluated using equation $S^0_{\mathbf{GG}'}(\mathbf{q},\omega)=-\frac{1}{\pi}{\rm sgn}(\omega){\rm Im}[\chi^o_{\mathbf{GG}'}(\mathbf{q},\omega)]$,[19] with the spectral function $S^0_{\mathbf{GG}'}(\mathbf{q},\omega)$ defined as

$$\begin{aligned}S^0_{\mathbf{GG}'}(\mathbf{q},\omega)=\frac{2}{\Omega}\sum_{\mathbf{k}}^{\rm BZ}\sum_{n}^{\rm occ}\sum_{n'}^{\rm unocc}&\delta(\varepsilon_{n\mathbf{k}}-\varepsilon_{n'\mathbf{k}+\mathbf{q}}+\omega)\\ &\times\langle\psi_{n\mathbf{k}}|e^{-{\rm i}(\mathbf{q}+\mathbf{G})\cdot\mathbf{r}}|\psi_{n'\mathbf{k}+\mathbf{q}}\rangle\\ &\times\langle\psi_{n'\mathbf{k}+\mathbf{q}}|e^{{\rm i}(\mathbf{q}+\mathbf{G}')\cdot\mathbf{r}}|\psi_{n\mathbf{k}}\rangle \qquad (2)\end{aligned}$$

and ${\rm Re}[\chi^o_{\mathbf{GG}'}(\mathbf{q},\omega)]$ is evaluated via the Kramers-Kronig relation using an energy cutoff of 50 eV. Here the $\mathbf{G}$'s are the reciprocal lattice vectors, n,n' are band indices, the wave vectors $\mathbf{k}$ and $\mathbf{q}$ are in the first Brillouin zone (BZ), the factor 2 accounts for the spin, and Ω is the normalization volume. In practice, we replace the δ-function in Eq. (2) by a Gaussian $\frac{1}{\sqrt{\pi}\gamma}e^{-\omega^2/\gamma^2}$ with a very small broadening parameter $\gamma=10$ meV. The sum over $\mathbf{k}$ was performed on a $108\times108\times360$ grid. The use of such a fine $\mathbf{k}$-mesh sampling is crucial to achieve convergence of dielectric properties in MgB_2 at low energies. The one-particle energies $\epsilon_{n\mathbf{k}}$ and wave functions $\psi_{n\mathbf{k}}$ are obtained as self-consistent solutions of Kohn-Sham equations using norm-conserving pseudopotentials[20] and the

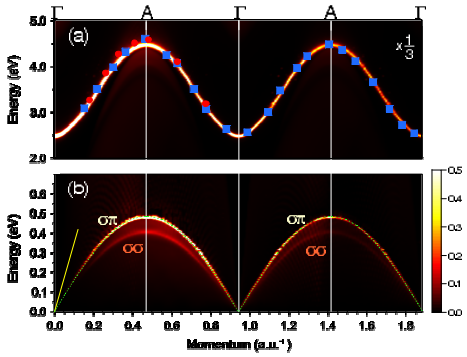

FIG. 1: (color). Calculated $-\mathrm{Im}[\epsilon^{-1}(q_c,\omega)]$ versus ω and q_c in two energy regions. Calculations include local-field effects and the RPA kernel. In (a) the circles and squares mark the energy-loss peak positions measured in x-ray scattering experiments of Refs. 24 and 25, respectively. In (b) the dispersion of the upper sharp $\sigma\pi$ plasmon peak is described by $\omega_{\sigma\pi} = V_{\sigma\pi}\cdot|\sin(\frac{c}{2}q_c)|$ (green dashed line) with $V_{\sigma\pi} = 0.48$ eV. The lower broad feature with similar sine-like dispersion corresponds to the $\sigma\sigma$ plasmon. Yellow solid line presents acoustic plasmon dispersion according to Ref. 32.

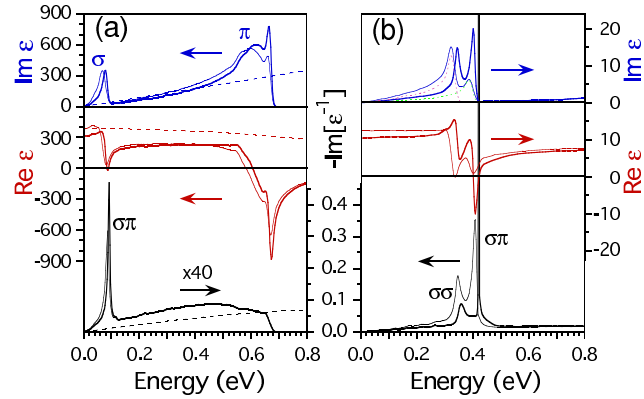

FIG. 2: (color). Real (red lines) and imaginary (blue lines) parts of the dielectric function, $\epsilon(q_c,\omega)$, and the corresponding loss function, $-\mathrm{Im}[\epsilon^{-1}(q_c,\omega)]$, (black lines) for (a) $q_c = 0.055$ a.u.$^{-1}$ and (b) $q_c = 0.322$ a.u.$^{-1}$ evaluated with the use of the RPA kernel. Thick (thin) lines stand for results with (without) inclusion of local-field effects. In (a) the dashed lines are the free-electron gas results for $r_s = 1.8$ a.u. In (b) thin dotted lines show contributions to Imϵ due to intraband transitions within the σ_1 (green) and σ_2 (purple) bands.

exchange-correlation potential of Ref. 21. In order to elucidate the role of exchange-correlation effects in the density-response function, we performed calculations of χ using two forms of the many-body kernel K_{xc}, namely the random-phase approximation (RPA) (K_{xc}=0), and an adiabatic extension of the local-density approximation (TDLDA).[22]

The calculated loss function, $-\mathrm{Im}[\epsilon^{-1}(\mathbf{q},\omega)]$,[23] directly probed in inelastic scattering experiments is presented in Fig. 1 as a function of the momentum transfer $\mathbf{q}$ along the c^* axis. In the upper energy range (Fig. 1a) it is dominated by a well-defined collective mode dispersing in the 2.5-4.5 eV energy range in excellent agreement with x-ray experiments.[24,25] The existence of this mode for momenta in the first BZ was demonstrated in Refs. 26 and 27, whereas its cosine-like oscillating dispersion in higher BZ's was recently discovered in a joint experimental-theoretical study.[25] This mode produces a strong impact on electrodynamical and optical properties[28,29,30] of MgB_2, however, it has no relevance to superconductivity as it affects neither the dynamically screened Coulomb interaction at low energies nor phonon dispersion.[27]

Figure 1b shows the calculated loss function in the low-energy domain that is our main finding. At all q_c it is dominated by a sharp "$\sigma\pi$" peak with a sine-like dispersion. Figure 2 shows the dielectric and loss functions at $q_c = 0.055$ a.u.$^{-1}$ and $q_c = 0.322$ a.u.$^{-1}$. One can see how the presence of two types of carriers (in the σ and π bands) around E_F (see Fig. 3a) with a large difference in the perpendicular component of the group velocity, $v^{\perp}$, (compare maximal $v^{\perp}$ in the π bands (Fig. 3b) with that in the σ bands (Figs. 3c and 3d)) produces in Imϵ a structure consisting of two main peaks (Fig. 2a). Thus, while the faster π carriers give rise to a broad structure from 0 to 0.68 eV in Fig. 2a with the main peak at the upper-energy side, the σ carriers which are moving more slowly in the c^* direction produce a sharp peak in the low-energy part of Imϵ. The reason of this sharpness resides in the fact that within both σ bands, the number of states with maximal $v^{\perp}$ is greatly enhanced as seen in Figs. 3c-3d. Therefore, the number of intra-band transitions involving these fast states is large which strongly enhances the σ peak in Imϵ at the higher energies. In turn, this causes a dramatic drop in Reϵ at nearly the same energy which, combined with the presence of a local minimum around $\omega = 0.1$ eV in Imϵ, produces a well-defined sharp peak in $-\mathrm{Im}[\epsilon^{-1}]$ corresponding to charge density fluctuations between the σ and π bands, a $\sigma\pi$ mode. Despite the presence of a non-vanishing value of Imϵ at the ω where the $\sigma\pi$ peak appears, its intrinsic width is extremely small, being in the meV range (which corresponds to a lifetime of few hundreds of femtoseconds), and is almost entirely determined by an extrinsic broadening parameter γ.

Since at small q_c the two main peaks in Imϵ disperse linearly with momentum according to their maximal perpendicular Fermi velocity components, $\mathrm{Im}\epsilon \propto v_{F,\max}^{\perp\sigma(\pi)}\cdot q_c$, the dispersion of the $\sigma\pi$ mode (linked to the upper side of the continuum for electron-hole excitations within the σ bands) is also linear in q_c and its group velocity $v_{\sigma\pi}$ is close to $v_{F,\max}^{\perp\sigma}$.[31] This corresponds to the acoustic plasmon proposed to exist in MgB_2 on the basis of a model tight-binding calculation.[32] The concept of an acoustic plasmon goes back to Pines[33] who showed that it can occur in a two-component electron plasma consisting of slow and fast carriers. The fast carriers (within the π bands in MgB_2) can act to screen the repulsion between slow carriers (within the σ bands in MgB_2) resulting in the appearance of a plasmon mode with a peculiar

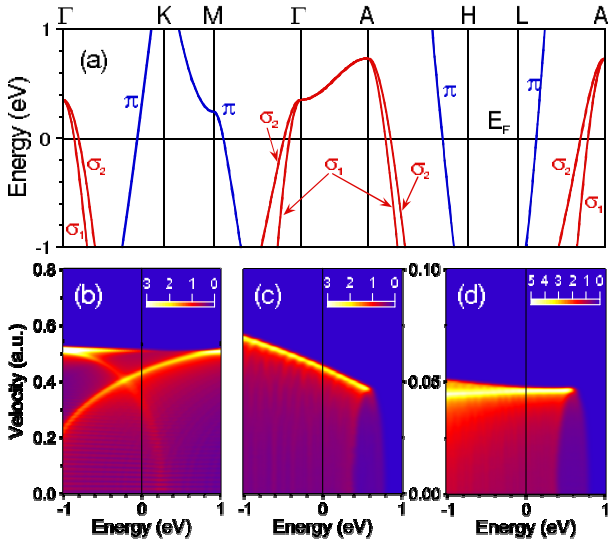

FIG. 3: (color). (a) Energy band structure of MgB_2 along some symmetry directions of the Brillouin zone in the vicinity of the Fermi level, E_F. Maps of the density of states in the π (b), σ_1 (c), and σ_2 (d) bands versus their energy and group velocity component along the c^* axis. Note the different velocity range of (b) in comparison with (c) and (d).

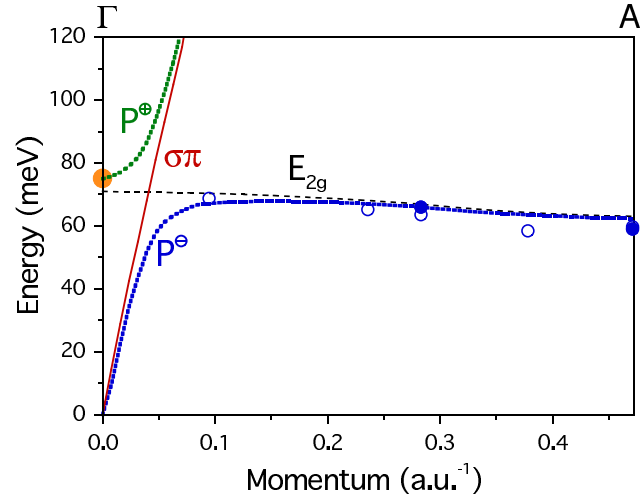

FIG. 4: (color online). The low-energy part of the bare $\sigma\pi$ plasmon (red solid line) along with the calculated[37] bare E_{2g}-phonon (dashed line) and measured peak positions (open[8] and filled[13] circles). The position of the Raman spectrum peak is shown by an orange filled circle at $q_c = 0$. Dispersions of the hybrid "$\sigma\pi - E_{2g}$" modes, $P^{\oplus}$ and $P^{\ominus}$, are shown by green and blue thick dotted lines, respectively. In the evaluation of these curves we use a "$\sigma\pi - E_{2g}$" coupling parameter Δ=17.3 meV in order to place the position of the $P^{\oplus}$ mode at $q_c = 0$ in agreement with the Raman measurements.[5,6,7]

sound-like dispersion. After the recognition of the role in the acoustic plasmon as a possible mechanism for superconductivity in transition metals,[34] it has been regularly evoked for explaining superconductivity in materials with unusually high T_c. Nevertheless, up to now the issue remains controversial since the very existence of such a collective mode in metals has been confirmed neither experimentally nor by *ab initio* calculations. Only recently an acoustic-like plasmon was observed in the electron energy-loss measurements at a metal surface in excellent agreement with the *ab initio* prediction,[35] thus greatly increasing our confidence in the present results.

With increasing q_c the σ peak in Imϵ, and consequently the $\sigma\pi$ peak in $-$Im$[\epsilon^{-1}]$, starts to split into two peaks (Figs. 1b and 2b) since for holes, $v_{\max}^{\perp\sigma_1}$ exceeds $v_{\max}^{\perp\sigma_2}$ by more than 20% (Figs. 3(c) and 3(d)). In this case the higher(lower)-energy plasmon peak in $-$Im$[\epsilon^{-1}]$ corresponds to the charge fluctuations between σ_1 and π (σ_1 and σ_2) bands. Whereas the $\sigma\pi$ plasmon continues to be long-lived, the lower-energy $\sigma\sigma$ plasmon has a significantly shorter lifetime due to more efficient scattering within the σ_1 band. We expect the two separate modes to exist at any q_c, however, when the calculated broadening γ exceeds the energy difference between these modes only a single $\sigma\pi$ peak arises in $-$Im$[\epsilon^{-1}]$ (Fig. 2a).[36]

In Fig. 1b one can see how with increasing q_c both of these plasmon modes reach maximum energy at the A point and, as momentum increases further, their dispersions change from positive to negative and approach $\omega = 0$ at the Γ point in the second BZ, in striking contrast to results of Ref. 32. The origin of this periodic behavior resides in the fact that strong local-field effects in MgB_2 feed the strength from the small q_c modes into the charge density fluctuations at large $(q_c + G_z)$ in a similar fashion as occurs in the case of the higher energy mode.[25] These sine-like dispersing modes continue to have strength at momenta in subsequent BZ's and this is a direct consequence of a layered MgB_2 structure. Additionally, as seen in Fig. 2, the local-field effects lead to a blue shift of the $\sigma\sigma$ and $\sigma\pi$ energy and make the $\sigma\pi$ peak more narrow as it occurs for ω corresponding to smaller Imϵ. We also analyzed the role of exchange-correlation effects beyond the RPA and found that the RPA picture is essentially sufficient for the description of low-energy collective excitations in MgB_2. The inclusion of the TDLDA kernel in the calculation of $\chi(q_c, \omega)$ leads to only a small (few percent) downward shift of the plasmon mode dispersions with a slight reduction of their lifetimes, i.e., in part compensating the local-field effects.

The $\sigma\pi$ plasmon can have deep impact on both low-energy-electron and phonon dynamics in MgB_2. Our calculation reveals dramatic modification of the dynamical Coulomb interaction in the energy range vital for superconductivity. In Fig. 2 one can see that in the neighborhood of the $\sigma\pi$ plasmon energy the calculated Re$[\epsilon(q_c, \omega)]$ differs dramatically from static $\epsilon(q_c, \omega = 0)$ as well as from the free electron gas result. In particular, in a certain momentum-energy phase space region, Reϵ is even negative leading to overall reduction of Coulomb repulsion between carriers. This could explain in part the observed reduced isotope effect in MgB_2.[2,3,4] It would be of great interest to quantify this effect within the *ab*

initio approach.[15] Note, that the $\sigma\pi$ plasmon does not influence inter-band σ-π and intra-band σ scattering due to the phase-space restrictions, although could have some effect in the intra-band π one.

The $\sigma\pi$ plasmon can dramatically affect the dispersion of the optical phonon modes in the "pathological" region of small $\mathbf{q}$,[13] offering an unexpected explanation of widely-discussed discrepancies between the Raman and x-ray measurements of the phonon structure in MgB_2. The ~ 77 meV peak observed in Raman-scattering experiments and commonly attributed to the boron E_{2g} phonon mode is always strongly renormalized in comparison with a bare phonon dispersion, whereas the x-ray experiments performed for large q_c do not see any appreciable renormalization. In Fig. 4 we show the calculated dispersion of the bare $\sigma\pi$ mode along with the bare E_{2g} phonon mode[37] compared to the experimental data.[8,13] One can see how the two bare curves cross each other close to the Γ point. Due to its localization in the boron plane the $\sigma\pi$ plasmon strongly interacts with the boron E_{2g} phonon mode resulting in strong hybridization of these boson modes. The result shown by green and blue dashed lines in Fig. 4 demonstrates that the mode seen in the Raman experiments is indeed a strongly hybridized "$\sigma\pi$-E_{2g}" $P^{\oplus}$ mode. Note, that the finite electron lifetime effect[11,14] can also contribute to the upward shift of this mode. Additionally, a steep $\sigma\pi$ plasmon dispersion at small momenta might explain the existence of the strong unstructured background (commonly mentioned as being of unknown electronic origin) observed in the Raman experiments. This is corroborated by the fact that, e.g., in AlB_2, where we do not expect the existence of such a plasmon, this background does not appear.[5,38]

In conclusion, our detailed *ab initio* calculation demonstrates the existence in MgB_2 in the 0-0.5 eV energy range of hitherto unknown long-lived collective mode that corresponds to coherent charge fluctuations between the boron $\sigma-$ and $\pi-$ bands ($\sigma\pi$ mode) with striking periodic sine-like dispersion. This mode shows an acoustic-like behavior at small momenta where it can strongly interact with optical phonons. Additionally we find at slightly lower energy a more strongly damped mode that corresponds to charge fluctuations between two different σ bands ($\sigma\sigma$ mode). Both these modes have profound impact on the low-energy dynamical Coulomb interaction which should be explicitly taken into account in *ab initio* theories of superconductivity to have the predictive power.

We acknowledge partial support from the University of the Basque Country (Grant No. GIC07IT36607), the Departamento de Educación del Gobierno Vasco, and the Spanish Ministerio de Ciencia y Tecnología (MCyT) (Grant No. FIS200766711C0101).

[1] J. Nagamatsu, N. Nakagawa, T. Muranaka, Y. Zenitani, and J. Akimitsu, Nature (London) **410**, 63 (2001).
[2] D. G. Hinks, H. Claus, and J. D. Jorgensen, Nature (London) **411**, 457 (2001).
[3] S. L. Bud'ko, G. Lapertot, C. Petrovic, C. E. Cunningham, N. Anderson, and P. C. Canfield, Phys. Rev. Lett. **86**, 1877 (2001).
[4] L. Simonelli, V. Palmisano, M. Fratini, M. Filippi, P. Parisiades, D. Lampakis, E. Liarokapis, and A. Bianconi, Phys. Rev. B **80**, 014520 (2009).
[5] K.-P. Bohnen, R. Heid, and B. Renker, Phys. Rev. Lett. **86**, 5771 (2001).
[6] A. F. Goncharov, V. V. Struzhkin, E. Gregoryanz, J. Hu, R. J. Hemley, H.-K. Mao, G. Lapertot, S. L. Bud'ko, and P. C. Canfield, Phys. Rev. B **64**, 100509(R) (2001).
[7] J. W. Quilty, S. Lee, A. Yamamoto, and S. Tajima, Phys. Rev. Lett. **88**, 087001 (2002).
[8] A. Shukla, M. Calandra, M. d'Astuto, M. Lazzeri, F. Mauri, Ch. Bellin, M. Krisch, J. Karpinski, S. M. Kazakov, J. Jun, D. Daghero, and K. Parlinski, Phys. Rev. Lett. **90**, 095506 (2003).
[9] A. Q. R. Baron, H. Uchiyama, Y. Tanaka, S. Tsutsui, D. Ishikawa, S. Lee, R. Heid, K.-P. Bohnen, S. Tajima, and T. Ishikawa, Phys. Rev. Lett. **92**, 197004 (2004).
[10] A. Q. R. Baron, H. Uchiyama, R. Heid, K. P. Bohnen, Y. Tanaka, S. Tsutsui, D. Ishikawa, S. Lee, and S. Tajima, Phys. Rev. B **75**, 020505(R) (2007).
[11] E. Cappelluti, Phys. Rev. B **73**, 140505(R) (2006).
[12] M. Calandra, M. Lazzeri, and F. Mauri, Physica C **456**, 38 (2007).
[13] M. d'Astuto, M. Calandra, S. Reich, A. Shukla, M. Lazzeri, F. Mauri, J. Karpinski, N. D. Zhigadlo, A. Bossak, and M. Krisch, Phys. Rev. B **75**, 174508 (2007).
[14] A. M. Saitta, M. Lazzeri, M. Calandra, and F. Mauri, Phys. Rev. Lett. **100**, 226401 (2008).
[15] A. Floris, G. Profeta, N. N. Lathiotakis, M. Lüders, M. A. L. Marques, C. Franchini, E. K. U. Gross, A. Continenza, and S. Massidda, Phys. Rev. Lett. **94**, 037004 (2005).
[16] J. Kortus, I. I. Mazin, K. D. Belashchenko, V. P. Antropov, and L. L. Boyer, Phys. Rev. Lett. **86**, 4656 (2001).
[17] J. M. An and W. E. Pickett, Phys. Rev. Lett. **86**, 4366 (2001).
[18] M. Petersilka, U. J. Gossmann, and E. K. U. Gross, Phys. Rev. Lett. **76**, 1212 (1996).
[19] F. Aryasetiawan and O. Gunnarsson, Phys. Rev. B **49**, 16214 (1994).
[20] N. Troullier and J. L. Martins, Phys. Rev. B **43**, 1993 (1991).
[21] D. M. Ceperley and B. J. Alder, Phys. Rev. Lett. **45**, 566 (1980).
[22] E. K. U. Gross, J. F. Dobson, and M. Petersilka, in *Density Functional Theory II*, edited by R. F. Nalewajski (Springer, Berlin, 1996).
[23] $\epsilon^{-1} \equiv \epsilon_{00}^{-1}$ is obtained from $\epsilon^{-1}_{\mathbf{GG'}}(\mathbf{q},\omega) = 1 + 4\pi/(\mathbf{q}+\mathbf{G})^2\chi_{\mathbf{GG'}}(\mathbf{q},\omega)$ evaluated with the use of 25 $\mathbf{G}$ vectors.
[24] S. Galambosi, J. A. Soininen, A. Mattila, S. Huotari, S. Manninen, Gy. Vankó, N. D. Zhigadlo, J. Karpinski, and K. Hämäläinen, Phys. Rev. B **71** 060504 (2005).
[25] Y. Q. Cai, P. C. Chow, O. D. Restrepo, Y. Takano, K. Togano, H. Kito, H. Ishii, C. C. Chen, K. S. Liang, C. T.

Chen, S. Tsuda, S. Shin, C. C. Kao, W. Ku, and A. G. Eguiluz, Phys. Rev. Lett. **97**, 176402 (2006).
[26] V. P. Zhukov, V. M. Silkin, E. V. Chulkov, and P. M. Echenique, Phys. Rev. B **64**, 180507(R) (2001).
[27] W. Ku, W. E. Pickett, R. T. Scalettar, and A. G. Eguiluz, Phys. Rev. Lett. **88**, 057001 (2002).
[28] T. Kakeshita, S. Lee, and S. Tajima, Phys. Rev. Lett. **97**, 037002 (2006).
[29] V. Guritanu, A. B. Kuzmenko, D. van der Marel, S. M. Kazakov, N. D. Zhigadlo, and J. Karpinski, Phys. Rev. B **73**, 104509 (2006).
[30] A. B. Kuzmenko, Physica C **456**, 63 (2007).
[31] In the present numerical calculations this has been demonstrated down to the energy $\omega \sim 25$ meV.
[32] K. Voelker, V. I. Anisimov, and T. M. Rice, arXiv:cond-mat/0103082 (unpublished).
[33] D. Pines, Can. J. Phys. **34**, 1379 (1956).
[34] H. Fröhlich, J. Phys. C **1**, 544 (1968).
[35] B. Diaconescu, K. Pohl, L. Vattuone, L. Savio, Ph. Hofmann, V. M. Silkin, J. M. Pitarke, E. V. Chulkov, P. M. Echenique, D. Farías, and M. Rocca, Nature (London) **448**, 57 (2007).
[36] Thus, the usage of $\gamma = 100$ meV leads to the occurrence of a broad single $\sigma\pi$ peak at all q_c only: A. Balassis, E. V. Chulkov, P. M. Echenique, and V. M. Silkin, Phys. Rev. B **78**, 224502 (2008).
[37] T. Yildirim, O. Gülseren, J. W. Lynn, C. M. Brown, T. J. Udovic, Q. Huang, N. Rogado, K. A. Regan, M. A. Hayward, J. S. Slusky, T. He, M. K. Haas, P. Khalifah, K. Inumaru, and R. J. Cava, Phys. Rev. Lett. **87**, 037001 (2001).
[38] B. Renker, K. B. Bohnen, R. Heid, D. Ernst, H. Schober, M. Koza, P. Adelmann, P. Schweiss, and T. Wolf, Phys. Rev. Lett. **88**, 067001 (2002).